

PAMPAC: A Parallel Adaptive Method for Pseudo-Arclength Continuation

D.A. Aruliah, University of Ontario Institute of Technology
 Lennaert van Veen, University of Ontario Institute of Technology
 Alex Dubitski, Amadeus R&D, Toronto

Pseudo-arclength continuation is a well-established method for generating a numerical curve approximating the solution of an underdetermined system of nonlinear equations. It is an inherently sequential predictor-corrector method in which new approximate solutions are extrapolated from previously converged results and then iteratively refined. Convergence of the iterative corrections is guaranteed only for sufficiently small prediction steps. In high-dimensional systems, corrector steps are extremely costly to compute and the prediction step-length must be adapted carefully to avoid failed steps or unnecessarily slow progress. We describe a parallel method for adapting the step-length employing several predictor-corrector sequences of different step lengths computed concurrently. In addition, the algorithm permits intermediate results of unconverged correction sequences to seed new predictions. This strategy results in an aggressive optimization of the step length at the cost of redundancy in the concurrent computation. We present two examples of convoluted solution curves of high-dimensional systems showing that speed-up by a factor of two can be attained on a multi-core CPU while a factor of three is attainable on a small cluster.

Categories and Subject Descriptors: G.1.5 [Numerical Analysis]: Roots of Nonlinear Equations—Continuation (homotopy) methods; G.4 [Mathematical Software]: Parallel and Vector Implementations

General Terms: Algorithms, Performance

Additional Key Words and Phrases: Pseudo-arclength Continuation, Parallel Computing, Adaptivity

ACM Reference Format:

Aruliah, D. A., van Veen, L., Dubitski, A. 2012. PAMPAC: A Parallel Adaptive Method for Pseudo-Arclength Continuation. *ACM Trans. Math. Softw.* 0, 0, Article 0 (2012), 21 pages.

DOI = 10.1145/0000000.0000000 <http://doi.acm.org/10.1145/0000000.0000000>

1. INTRODUCTION

Continuation or *homotopy* problems arise naturally in numerous application domains. They are used to study the parameter-dependence of solutions of nonlinear problems by continuously morphing between different systems of equations. For instance, in the numerical study of the Navier-Stokes equations for fluid motion, the Reynolds number Re often appears as a parameter. Certain computations—*e.g.*, those of time-periodic solutions or travelling waves—are significantly less challenging at low Reynolds numbers than at high Reynolds numbers where dynamical processes occur on a larger range of spatial scales. Continuation can be used to extend the results obtained at some low Reynolds number into the physically more interesting regime by constructing a homotopy between turbulent flows with distinct characteristics. Homotopies are

This work is supported by the Natural Sciences and Engineering Research Council. Author's addresses: Faculty of Science, UOIT, 2000 Simcoe Street North, Oshawa, ON, L1H 7K4

Permission to make digital or hard copies of part or all of this work for personal or classroom use is granted without fee provided that copies are not made or distributed for profit or commercial advantage and that copies show this notice on the first page or initial screen of a display along with the full citation. Copyrights for components of this work owned by others than ACM must be honored. Abstracting with credit is permitted. To copy otherwise, to republish, to post on servers, to redistribute to lists, or to use any component of this work in other works requires prior specific permission and/or a fee. Permissions may be requested from Publications Dept., ACM, Inc., 2 Penn Plaza, Suite 701, New York, NY 10121-0701 USA, fax +1 (212) 869-0481, or permissions@acm.org.

© 2012 ACM 0098-3500/2012/-ART0 \$10.00

DOI 10.1145/0000000.0000000 <http://doi.acm.org/10.1145/0000000.0000000>

also used to compute and contrast similarities and differences of flows in disparate geometries (see Kawahara et al. [2012] and references therein).

In mathematical terms, homotopy or continuation problems are nonlinear systems of equations where the number of equations is one fewer than the number of variables. That is, given a mapping $\mathbf{F} : \mathbb{R}^n \times \mathbb{R} \rightarrow \mathbb{R}^n$, the equation

$$\mathbf{F}(\mathbf{x}, \lambda) = \mathbf{0} \quad (1)$$

with vector $\mathbf{x} \in \mathbb{R}^n$ and scalar $\lambda \in \mathbb{R}$ defines a continuation problem. In geometric terms, Eq. (1) implicitly defines a one-dimensional curve in \mathbb{R}^{n+1} under suitable smoothness and consistency properties of the mapping \mathbf{F} .

The essential idea of continuation, or homotopy, is to follow this curve of solutions in (1). We assume the parameter λ lies in some specified interval $[\lambda_{\min}, \lambda_{\max}] \subseteq \mathbb{R}$. Often, the problem can be formulated so that solving Eq. (1) for \mathbf{x} is easy for some $\lambda^* \in [\lambda_{\min}, \lambda_{\max}]$ and that the goal is to obtain a solution \mathbf{x} when $\lambda = \lambda_{\min}$ or $\lambda = \lambda_{\max}$. Thus, continuation is the process of gradually morphing the solution of a straightforward problem into the solution of a formidable problem in small parameter increments.

Numerical continuation refers to families of numerical algorithms for generating points on the solution curve. Natural continuation and pseudo-arclength continuation are examples of predictor-corrector methods [Allgower and Georg 2003; Govaerts 2000; Kuznetsov 1998]. In the prediction stage, a putative new point on the curve is computed and, in the correction stage, the putative candidate is iteratively refined until a solution of (1) is found. Such algorithms are inherently sequential: previously computed points are used to predict the next solution point on the curve. Parallelization can be introduced within corrector iterations but the predictor steps need to be computed in sequence.

More importantly, predictor-corrector methods rely on adaptive step-size selection to make optimal progress in moving along the curve of solutions [Allgower and Georg 2003]. Strategies for adapting step-sizes selection are largely heuristic: when corrector steps fail to converge, the predictor step is rejected, the step-size is reduced, and a new prediction step is generated. This turns out to be the principal bottleneck in many continuation problems: computation time devoted to nonconvergent corrector steps is wasted. As such, identifying strategies to improve the performance of predictor-corrector schemes by reducing the cost of failed predictor steps is a significant challenge in modern High-Performance Computing for numerical continuation problems.

We describe in the present work a parallel software library and the underlying algorithms that extend adaptive predictor-corrector methods to amortize the cost of rejected predictor steps. Specifically, we compute several predictor steps of different step-sizes in parallel on distinct processors. At the same time, intermediate corrector iterates can seed new predictor steps. This strategy is most effective when corrector steps are costly. In particular, the time for a single corrector iteration should be much larger than the communication time between processors and should not depend sensitively on the step-size. Moreover, the curve defined by (1) should have curvature that varies dramatically so that the optimal continuation step-size also changes significantly along the solution curve.

2. BACKGROUND

We briefly review existing numerical continuation algorithms—notably natural parameter and pseudo-arclength continuation—before describing our parallel adaptive algorithm. The prototypical problem is of the form (1) where $\lambda \in [\lambda_{\min}, \lambda_{\max}] \subseteq \mathbb{R}$, $\mathbf{x} \in \mathbb{R}^n$ and $\mathbf{F} : \mathbb{R}^n \times \mathbb{R} \rightarrow \mathbb{R}^n$. We sometimes write the underlying equation (1) in the

form

$$\mathbf{F}(\mathbf{z}) = \mathbf{0}, \text{ where } \mathbf{z} = (\mathbf{x}, \lambda) \in \mathbb{R}^{n+1}. \quad (2)$$

That is, we treat the concatenation of the n -vector \mathbf{x} and the scalar λ as a single $(n + 1)$ -vector \mathbf{z} while using the same symbol \mathbf{F} to denote the mapping; technically, this notation is ambiguous but the meaning is clear from the context. Also, we denote appropriately-sized matrices representing Jacobian derivatives by

$$\mathbf{F}_\lambda \equiv \frac{\partial \mathbf{F}}{\partial \lambda} \in \mathbb{R}^{n \times 1}, \quad \mathbf{F}_\mathbf{x} \equiv \frac{\partial \mathbf{F}}{\partial \mathbf{x}} \in \mathbb{R}^{n \times n}, \quad \text{and} \quad \mathbf{F}_\mathbf{z} \equiv \frac{\partial \mathbf{F}}{\partial \mathbf{z}} \in \mathbb{R}^{n \times (n+1)} \quad \text{respectively.} \quad (3)$$

For concreteness, the goal is to find a vector $\mathbf{x} = \mathbf{x}(\lambda_{\max})$ satisfying $\mathbf{F}(\mathbf{x}(\lambda_{\max}), \lambda_{\max}) = \mathbf{0}$ when λ initially starts from $\lambda^* = \lambda_{\min}$ (that is, the curve is traversed with λ increasing, at least initially). As a first obvious method for constructing the numerical curve of solutions, one can increment the parameter λ gradually from λ_{\min} to λ_{\max} . That is, given a point $(\mathbf{x}, \lambda) \in \mathbb{R}^{n+1}$ known to lie on the curve, a new point on the curve $(\boldsymbol{\xi}, \lambda + h)$ is found

- (1) by incrementing λ by a small amount $h > 0$; and
- (2) by solving the n equations $\mathbf{F}(\boldsymbol{\xi}, \lambda + h) = \mathbf{0}$ for the unknown $\boldsymbol{\xi} \in \mathbb{R}^n$.

This approach is referred to as *natural parameter continuation* (or, more simply, *natural continuation*) [Allgower and Georg 2003; Govaerts 2000; Kuznetsov 1998]. Algorithm 1 is a high-level description of natural continuation. Fixing the known parameter value $\lambda \mapsto \lambda + h$ in the underdetermined nonlinear system $\mathbf{F}(\boldsymbol{\xi}, \lambda) = \mathbf{0}$ yields a closed $n \times n$ system in the n unknown components of $\boldsymbol{\xi}$. Intuitively, if h is sufficiently small, the vector $\boldsymbol{\xi}$ should be easy to obtain using a quadratically-convergent Newton iteration (see, e.g., Kelley [2003]).

ALGORITHM 1: Natural parameter continuation.

Input: $[\lambda_{\min}, \lambda_{\max}] \subseteq \mathbb{R}$; vector $\mathbf{x}^{(0)} \in \mathbb{R}^n$ where $\mathbf{F}(\mathbf{x}^{(0)}, \lambda_{\min}) = \mathbf{0}$; step-size $h > 0$
Output: vector $\mathbf{x}^{(k)} \in \mathbb{R}^n$ and scalar $\lambda^{(k)} \geq \lambda_{\max}$ such that $\mathbf{F}(\mathbf{x}^{(k)}, \lambda^{(k)}) = \mathbf{0}$

```

1  $k \leftarrow 0$ 
2  $\lambda^{(0)} \leftarrow \lambda_{\min}$                                      % initialization
3 while  $\lambda^{(k)} < \lambda_{\max}$  do                             % loop to generate successive points on curve
4      $\lambda \leftarrow \lambda^{(k)} + h$                          % predictor step
5     Iteratively solve  $n \times n$  nonlinear system of equations
                                      $\mathbf{F}(\boldsymbol{\xi}, \lambda) = \mathbf{0}$ 
        to obtain  $\boldsymbol{\xi} \in \mathbb{R}^n$  starting from initial iterate  $\boldsymbol{\xi}^{(0)} = \mathbf{x}^{(k)}$  % corrector steps
6     if iteration in line 5 converges to  $\boldsymbol{\xi}$  then           % accept next point on curve
7          $\mathbf{x}^{(k+1)} \leftarrow \boldsymbol{\xi}$ 
8          $\lambda^{(k+1)} \leftarrow \lambda$ 
9          $k \leftarrow k + 1$ 
10    else
11        Reduce step-size  $h$                                  % reject predictor step & repeat
12 return  $\mathbf{x}^{(k)}, \lambda^{(k)}$ 

```

Natural continuation is conceptually simple and easy to implement; however, it breaks down when the solution curve admits a *fold point* (i.e., a point (\mathbf{x}, λ) where the Jacobian matrix $\mathbf{F}_\mathbf{x}(\mathbf{x}, \lambda)$ is singular; see Dickson et al. [2007] for an alternative

characterization of fold points). At a fold point, systematically incrementing λ as in Algorithm 1 yields an inconsistent system of nonlinear equations that cannot be solved regardless of how small h is. Fold points do occur in practical continuation problems so other continuation strategies need to be devised [Yang and Keller 1986; Doedel et al. 2008].

Pseudo-arclength continuation (as outlined in Algorithm 2; see Allgower and Georg [2003]; Dickson et al. [2007]; Keller [1977]) is a standard approach to circumvent fold point singularities. Under the assumption that both \mathbf{x} and λ are smooth functions of arclength, pseudo-arclength continuation uses the unit direction $\mathbf{T} \in \mathbb{R}^{n+1}$ tangent to the curve for prediction. The term “pseudo-arclength” applies because the step-size h —i.e., the Euclidean distance in \mathbb{R}^{n+1} between successive points on the numerical curve—approximates the arclength as measured along the curve. The tangent direction \mathbf{T} can be determined by computing a null vector of the $n \times (n + 1)$ Jacobian matrix \mathbf{F}_z or by computing finite differences between successive points on the curve [Allgower and Georg 2003]. The underdetermined nonlinear system of equations (1) is then closed by requiring that the solution (\mathbf{x}, λ) sought must lie in the hyperplane orthogonal to the tangent direction \mathbf{T} at distance h from the last known point; see line 7 of Algorithm 2.

ALGORITHM 2: Pseudo-arclength continuation.

Input: $[\lambda_{\min}, \lambda_{\max}] \subseteq \mathbb{R}$; vector $\mathbf{x}^{(0)} \in \mathbb{R}^n$ where $\mathbf{F}(\mathbf{x}^{(0)}, \lambda_{\min}) = \mathbf{0}$; step-size $h > 0$
Output: vector $\mathbf{x}^{(k)} \in \mathbb{R}^n$ and scalar $\lambda^{(k)} \geq \lambda_{\max}$ such that $\mathbf{F}(\mathbf{x}^{(k)}, \lambda^{(k)}) = \mathbf{0}$

- 1 $k \leftarrow 0$
- 2 $\lambda^{(0)} \leftarrow \lambda_{\min}$ % initialization
- 3 $\mathbf{z}^{(0)} \leftarrow (\mathbf{x}^{(0)}, \lambda^{(0)}) \in \mathbb{R}^{n+1}$
- 4 Determine approximate tangent vector $\mathbf{T}^{(0)} \in \mathbb{R}^{n+1}$ at $\mathbf{z}^{(0)}$
- 5 **while** $\lambda^{(k)} < \lambda_{\max}$ **do** % loop to generate successive points on curve
- 6 $\mathbf{w} \leftarrow \mathbf{z}^{(k)} + h\mathbf{T}^{(k)}$ % predictor step
- 7 Iteratively solve $(n + 1) \times (n + 1)$ nonlinear system of equations

$$\begin{aligned} \mathbf{F}(\zeta) &= \mathbf{0}, \\ \mathbf{T}^{(k)T} (\zeta - \mathbf{z}^{(k)}) &= h \end{aligned}$$
- 8 to obtain $\zeta \in \mathbb{R}^{n+1}$ starting from initial iterate $\zeta^{(0)} = \mathbf{w}$ % corrector steps
- 9 **if** iteration in line 7 converges to ζ **then** % accept next point on curve
- 10 $\mathbf{x}^{(k+1)} \leftarrow \zeta_{1:n}$ % extract subvector from ζ
- 11 $\lambda^{(k+1)} \leftarrow \zeta_{n+1}$ % extract last element from ζ
- 12 $\mathbf{z}^{(k+1)} \leftarrow (\mathbf{x}^{(k+1)}, \lambda^{(k+1)})$
- 13 Determine approximate tangent vector $\mathbf{T}^{(k+1)} \in \mathbb{R}^{n+1}$ at $\mathbf{z}^{(k+1)}$
- 14 Heuristically adjust the step-size h
- 15 $k \leftarrow k + 1$
- 16 **else**
- 17 Reduce step-size h % reject predictor step \mathbf{w} and repeat
- 18 **return** $\mathbf{z}^{(k)} = (\mathbf{x}^{(k)}, \lambda^{(k)})$

Both natural continuation and pseudo-arclength continuation fit into a broader framework of *predictor-corrector methods* [Allgower and Georg 2003]. Predictor-corrector methods involve three important components:

- a *predictor step* of a prescribed step-size;
- a sequence of *corrector steps* (alternatively *corrector iterations*); and
- an adaptive step-size selection strategy.

The predictor step is used to seed the iterative solution of a nonlinear system of equations (successive iterates being called corrector steps). There are a variety of ways in which the predictor and corrector steps can be chosen; see Allgower and Georg [2003]; Doedel et al. [2008]. For instance, the predictor step in natural continuation comprises incrementing the scalar λ by h ; in pseudo-arclength continuation, prediction involves traversing a distance h along \mathbf{T} , the direction tangent to the curve. Whatever the particular predictor-corrector strategy, when the step-size h is too large, the inner corrector iterations can stagnate or diverge (either because the initial predictor is too far from a solution or perhaps because the system is inconsistent). In either event, the predictor step is rejected and the step-size is reduced according to a simple heuristic such as $h \leftarrow th$ where t is a user-specified parameter satisfying $0 < t < 1$. Consult [Allgower and Georg 2003, Ch. 6] for more detailed strategies for adapting step-sizes.

The structure of predictor-corrector methods has two significant consequences:

- (1) *The most expensive part of the algorithm is computation of the corrector steps* (especially when each iteration requires the solution of a linear system of equations as in, e.g., Newton’s method).
- (2) *Rejected predictor steps are costly* because numerous corrector steps are computed prior to rejection.

For moderate-sized nonlinear systems, the linear systems to be solved at each corrector iteration are amenable to dense, direct linear algebra solvers (e.g., as found in LAPACK libraries [Anderson et al. 1999]); as such, failed predictor steps may not be so punitive. However, for large-scale systems, time (and possibly memory) requirements for each corrector iteration grows algebraically, so using direct solvers becomes infeasible. In that case, *Krylov subspace iterations* (see, e.g., [Saad and Schultz 1986]) can be applied within Newton iterations to determine the corrector steps within a continuation algorithm. This process is referred to as *Newton-Krylov continuation* [Sánchez et al. 2004; Knoll and Keyes 2004]. The convergence of Krylov subspace methods depends critically on the properties of the Jacobian matrix and may require preconditioning. For certain problems with upward from 10,000 degrees of freedom, individual corrector steps in systems can require hours (in some cases, days) of computation—even using a well-tuned Krylov subspace method—and the penalty incurred for failed predictor steps is prohibitive. Given that rejected predictor steps can result from using a large step-size, an obvious strategy is to use very small step-sizes. Unfortunately, using small step-sizes impedes progress along the curve from λ_{\min} to λ_{\max} , both in natural and in pseudo-arclength continuation. Thus, efficient step-size adaptivity requires trading off between these conflicting concerns.

To achieve this balance, we develop a parallel software library—PAMPAC, a Parallel Adaptive Method for Pseudo-Arclength Continuation—that permits adaptive step-size selection within the predictor-corrector framework of pseudo-arclength continuation. The parallel algorithm implemented can be used for different kinds of correction steps and leads to speed-up for problems in which the computation of a correction iteration takes much longer than communication between processors. It is particularly effective for continuation problems in which the solution curve exhibits large variations in curvature (i.e., where the optimal step-size changes wildly along the curve).

3. SCHEME FOR PARALLELIZATION

There are two essential ways to achieve parallelism in the selection of step-sizes for predictor steps. The first is most obvious: use a concurrent sequence of predictor steps of different step-sizes t_1h, t_2h, \dots, t_Wh for some prescribed positive scalars $\{t_\alpha\}_{\alpha=1}^W$. That is, given W processes, an initial point $\mathbf{z} \in \mathbb{R}^{n+1}$ known to satisfy $\mathbf{F}(\mathbf{z}) = \mathbf{0}$ up to some fixed tolerance, and a unit tangent direction $\mathbf{T} \in \mathbb{R}^{n+1}$, each process α computes a predictor step $\zeta_\alpha^{(0)} = \mathbf{z} + t_\alpha h \mathbf{T}$. A maximum step-size h_{\max} may have to be set to avoid spurious convergence to a remote branch of the continuation curve; in that instance, fewer than W predictor steps would be computed. Once a prediction $\zeta_\alpha^{(0)}$ is determined by process α , the process computes a sequence of corrector steps $\{\zeta_\alpha^{(0)}, \zeta_\alpha^{(1)}, \zeta_\alpha^{(2)}, \dots\}$. Subsequent corrector iterations do not require inter-process communications and thus can be carried out concurrently by distinct processes. Each process α maintains its own iteration counter ν_α as well as the iterates $\zeta_\alpha^{(\nu_\alpha)}$ and the associated nonlinear residuals $\mathbf{r}_\alpha^{(\nu_\alpha)} \equiv \mathbf{F}(\zeta_\alpha^{(\nu_\alpha)})$.

A second strategy for parallel step-size adaptivity is to use intermediate computations to seed new predictions. That is, suppose process α is initialized using the predictor $\zeta_\alpha^{(0)} = \mathbf{z}_\alpha + h_\alpha \mathbf{T}_\alpha$ and proceeds to compute a sequence of correction steps $\{\zeta_\alpha^{(0)}, \zeta_\alpha^{(1)}, \zeta_\alpha^{(2)}, \dots\}$. Rather than waiting for the corrector iterations to converge, the intermediate iterates can be used to compute a normalized secant direction $\widehat{\mathbf{T}}_\alpha$ in the direction of $\zeta_\alpha^{(\nu_\alpha)} - \mathbf{z}_\alpha$ for some iterate ν_α . Assuming the corrector iterates are sufficiently close to the curve of solutions, the new secant direction $\widehat{\mathbf{T}}_\alpha$ approximates a tangent to the curve and can be handed off to another process β to generate a new predictor point $\mathbf{z}_\beta + h_\beta \mathbf{T}_\beta$, where $\mathbf{z}_\beta = \zeta_\alpha^{(\nu_\alpha)}$, $h_\beta = t_\ell h_\alpha$ for some $\ell \in \{1, \dots, W\}$, and $\mathbf{T}_\beta = \widehat{\mathbf{T}}_\alpha$.

To manage concurrent processes when both these strategies are employed, we represent each process by a node in a rooted tree with a master process at the root. The user specifies the tree's width $W > 0$ and depth $D > 0$; the width corresponds to the number of scalars t_1, t_2, \dots, t_W that multiply the step-length h and the depth corresponds to the number of extrapolated predictor steps computed from intermediate corrector iterates. New nodes, *i.e.*, new corrector sequences, are seeded only if physical processors are available; the queuing of multiple processes on a single processor hinders the continuation.

Each node in the tree corresponds to a potential computational process. A node α is associated with a current iteration counter ν_α and a current corrector iterate $\zeta_\alpha^{(\nu_\alpha)} \in \mathbb{R}^{n+1}$. The node α is generated with

$$\nu_\alpha \leftarrow 0 \text{ and } \zeta_\alpha^{(0)} \leftarrow \mathbf{z}_\alpha^{\text{init}} + h_\alpha^{\text{init}} \mathbf{T}_\alpha^{\text{init}}, \quad (4)$$

where the data $\mathbf{z}_\alpha^{\text{init}}$, $\mathbf{T}_\alpha^{\text{init}}$, and h_α^{init} are determined from the parent node (*i.e.*, the previous point on or near the continuation curve). When created, the node α also records ν_α^{init} —the number of corrector iterations that its parent had computed prior to spawning node α .

Node α also maintains a real parameter h_α representing the base step-size node that α uses to construct new predictor steps. Initially, $h_\alpha \leftarrow h_\alpha^{\text{init}}$, *i.e.*, the base step-size node α uses to make predictor steps is the same as the step-size used to initialize node α . However, in the event that all child nodes spawned from α lead to divergent sequences, h_α is reduced by some constant scaling factor $t \in (0, 1)$ before spawning more predictions. The scaling factor t is fixed to ensure all new prediction steps are at

a distance shorter than the shortest of the steps that just failed:

$$t = 0.9 \frac{t_{\min}}{t_{\max}}, \text{ where } t_{\min} = \min_{1 \leq k \leq W} t_k \text{ and } t_{\max} = \max_{1 \leq k \leq W} t_k.$$

This precaution ensures new predictors generated do not repeat earlier computations (after the failed child nodes are all deleted). If the base step-size h_{α_r} of the root node is reduced below some user-specified threshold H_{\min} , the continuation algorithm halts.

Each node α is assigned a color $c_\alpha \in \{\text{GREEN}, \text{YELLOW}, \text{RED}, \text{BLACK}\}$ as the algorithm proceeds. The color c_α of node α is determined using $\|\mathbf{r}_\alpha^{(\nu_\alpha)}\|_2$, *i.e.*, the 2-norm of the nonlinear residual $\mathbf{r}_\alpha^{(\nu_\alpha)} = \mathbf{F}(\zeta_\alpha^{(\nu_\alpha)}) \in \mathbb{R}^n$ at the current corrector iterate $\zeta_\alpha^{(\nu_\alpha)}$. Given positive parameters TOL_RESIDUAL , GAMMA , and MU , the rules are as follows:

- (1) $c_\alpha \leftarrow \text{GREEN}$ if $\|\mathbf{r}_\alpha^{(\nu_\alpha)}\|_2 \leq \text{TOL_RESIDUAL}$ (*i.e.*, the current iterate $\zeta_\alpha^{(\nu_\alpha)}$ is deemed to have converged to a point on or sufficiently near the solution curve);
- (2) $c_\alpha \leftarrow \text{YELLOW}$ if $\|\mathbf{r}_\alpha^{(\nu_\alpha)}\|_2^{\text{GAMMA}} \leq \text{TOL_RESIDUAL}$ (*i.e.*, the *next* iterate $\zeta_\alpha^{(\nu_\alpha+1)}$ is expected to have converged);
- (3) $c_\alpha \leftarrow \text{BLACK}$ if $\nu_\alpha > \text{MAX_ITER}$ or $\|\mathbf{r}_\alpha^{(\nu_\alpha)}\|_2 > \text{MU} \|\mathbf{r}_\alpha^{(\nu_\alpha-1)}\|_2$ (*i.e.*, the maximum number of corrector iterations is exceeded or the reduction of the residual is insufficient in consecutive corrector iterations); and
- (4) $c_\alpha \leftarrow \text{RED}$ otherwise.

The efficiency of the parallelization depends on the preceding criteria for coloring nodes.

New nodes are colored RED by default; the colors are reassessed after the current corrector iterates and the corresponding nonlinear residuals are computed on every node. The specific criteria for coloring a node GREEN, YELLOW, or BLACK depend on the nature of the corrector steps and the continuation problem at hand. As elucidated in Sec. 4, the user chooses these criteria by providing problem-dependent parameters TOL_RESIDUAL , MAX_ITER , GAMMA , and MU . The parameters TOL_RESIDUAL and MAX_ITER are standard as expected in any iterative solver. The other parameters GAMMA and MU are based on the asymptotic behavior of the user's choice of corrector sequences. For instance, when using Newton's method for corrector steps, we expect the decrease in the residual to be quadratic (or at least superlinear) near the solution curve; in that case, it makes sense to choose $\text{GAMMA} \in (1, 2)$ in the criterion (2) to color "nearly converged nodes" YELLOW. For predictor steps too far from the solution curve, we often see linear convergence only; it makes sense, then, to choose $\text{MU} \in (0, 1)$ in the criterion (3) to color a node BLACK when it is not converging sufficiently quickly. Nodes colored BLACK get deleted from the tree since computing more corrector steps likely leads to divergence or spurious convergence on another branch of the continuation curve.

Algorithm 3 is a high-level summary of the essential steps underlying our parallel adaptive algorithm. The main conceptual pieces are the concurrent computation of corrector steps from predictor steps of various step-lengths, extrapolation from intermediate corrector steps, and management of the parallel computations using a rooted tree with colored nodes.

The outermost loop of Algorithm 3 corresponds to accepting and logging valid points along the continuation curve. The nested loop spanning lines 3 to 9 describe the generation of new predictor points and their distribution over available processors. The processors compute individual corrector steps concurrently in line 9 requiring synchronization before advancing to line 10. This implies that the parallelization scheme

ALGORITHM 3: Essential parallel adaptive algorithm

Input: $[\lambda_{\min}, \lambda_{\max}] \subseteq \mathbb{R}$; vector $\mathbf{x}^* \in \mathbb{R}^n$ where $\mathbf{F}(\mathbf{x}^*, \lambda_{\min}) = \mathbf{0}$; step-size $h \neq 0$; tangent direction $\mathbf{T}^* \in \mathbb{R}^{n+1}$ where $\|\mathbf{T}^*\|_2 = 1$; tolerance $\text{TOL_RESIDUAL} > 0$; $\text{GAMMA} > 0$; $\text{MU} > 0$; depth $D > 0$; width $W > 0$; positive scaling parameters $\{t_1, t_2, \dots, t_W\}$

Output: vector $\mathbf{x}^{(k)} \in \mathbb{R}^n$ and scalar $\lambda^{(k)} \geq \lambda_{\max}$ such that $\mathbf{F}(\mathbf{x}^{(k)}, \lambda^{(k)}) = \mathbf{0}$

- 1 Seed root node α_r with data $(\mathbf{z}_{\alpha_r}, \hat{\mathbf{T}}_{\alpha_r}, h_{\alpha_r}) \leftarrow ((\mathbf{x}^*, \lambda_{\min}), \mathbf{T}^*, h)$ % initialization
- 2 **repeat** % loop to generate successive points on curve
- 3 **foreach** leaf node α **do** % Spawn new nodes
- 4 **if** depth of $\alpha < D$ **then**
- 5 **if** $\alpha \neq \alpha_r$ **then**
- 6 $\hat{\mathbf{T}}_{\alpha}^{\text{init}} \leftarrow \left\| \zeta_{\alpha}^{(\nu_{\alpha})} - \mathbf{z}_{\alpha}^{\text{init}} \right\|_2^{-1} (\zeta_{\alpha}^{(\nu_{\alpha})} - \mathbf{z}_{\alpha}^{\text{init}})$ % secant direction
- 7 **for** $\ell = 1 : W$ **do**
- 8 **if** processors are available **then**
- 9 Assign processor β_{ℓ} the data

$$\mathbf{z}_{\beta_{\ell}}^{\text{init}} \leftarrow \zeta_{\alpha}^{\nu_{\alpha}}, \quad \hat{\mathbf{T}}_{\beta_{\ell}}^{\text{init}} \leftarrow \hat{\mathbf{T}}_{\alpha}, \quad h_{\beta_{\ell}}^{\text{init}} \leftarrow t_{\ell} h_{\alpha}, \quad \nu_{\beta_{\ell}}^{\text{init}} \leftarrow \nu_{\alpha},$$

$$\nu_{\beta_{\ell}} \leftarrow 0, \quad \zeta_{\beta_{\ell}}^{(0)} \leftarrow \zeta_{\alpha}^{\nu_{\alpha}} + t_{\ell} h_{\alpha} \hat{\mathbf{T}}_{\alpha}, \quad c_{\beta_{\ell}} \leftarrow \text{RED}$$
- 10 Compute single corrector steps concurrently on all RED and YELLOW nodes of the tree.
- 11 Traverse nodes of tree updating residuals

$$\mathbf{r}_{\alpha}^{(\nu_{\alpha})} \leftarrow \mathbf{F}(\zeta_{\alpha}^{(\nu_{\alpha})})$$
- and updating colors c_{α} accordingly.
- 12 PruneTree(α_r), deleting BLACK nodes and eliminating redundant subtrees.
- 13 **while** root node α_r has a single child, β , and β is GREEN **do** % update root
- 14 Write the solution on α_r to disk
- 15 Update root: $\alpha_r \leftarrow \beta$
- 16 **until** root node α_r has $\lambda^{(\alpha_r)} \geq \lambda_{\max}$

is efficient only when the time required for a corrector step is much greater than the communication costs and when the time for the concurrent corrector computations is roughly the same on all processors. At a high level, the algorithm is mostly straightforward; further explanation is required to understand the pruning algorithm in line 12.

Concurrent computations are managed by pruning the tree in two stages. In the first stage, all subtrees rooted at BLACK nodes are removed. The corrector sequences associated with BLACK nodes are deemed to have made insufficient progress; as such, computing more corrector steps likely leads to divergence or spurious convergence to a point on another branch of the continuation curve. Other non-BLACK nodes are unaltered in this first stage.

Figure 1 provides a graphical illustration of the first stage of pruning. In panel (A), the GREEN root node represents a valid solution point with three child nodes (one YELLOW and two RED nodes). In panel (B), a concurrent corrector step is computed for all YELLOW and RED nodes (requiring 12 active processes in this case). At the end of the corrector step, four nodes are now GREEN, two are YELLOW, and four are BLACK. The first stage of pruning is simply to delete all BLACK nodes and their associated subtrees which leads to the configuration shown in panel (C).

The second stage of pruning—line 12 of Algorithm 3—involves comparing child nodes of a given parent node with viable corrector iterates and deciding which to

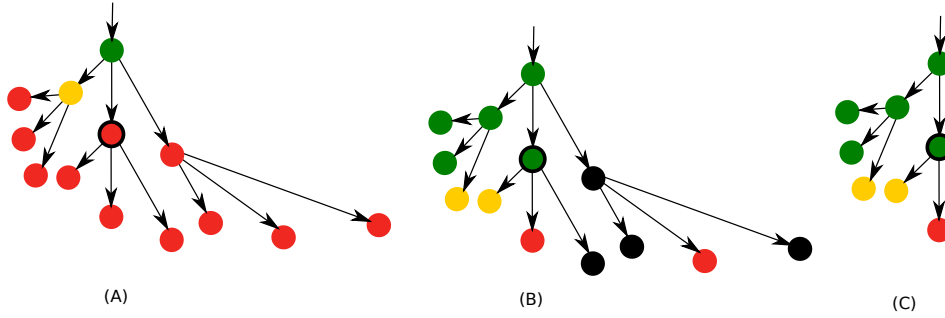


Fig. 1. Illustration of the first stage of the pruning algorithm on a tree of width 3 and depth 3. The links are drawn from left to right in the order of increasing step length. (A) GREEN root node representing a valid solution point and two levels of child nodes. Each of the nodes at depth 2 has three RED child nodes that have not done computed and corrector iterations as of yet. In (B), concurrent corrector steps have been computed on all YELLOW and RED nodes. After computing and assessing the residuals on all of the nodes, some have been colored GREEN (converged), YELLOW (almost converged), BLACK (diverged), or RED (undecided). In (C), all the BLACK nodes and their attached subtrees have been deleted.

keep and which to delete (along with associated subtrees). Doing so permits allocation of computing resources to nodes that are deemed to yield the greatest benefit. The greatest gain is determined by balancing the longest distance travelled along the continuation curve (*i.e.*, pseudoarclength) against the least amount of computational work (measured in corrector iterations). RED child nodes are kept by default—it is unclear whether they will yield convergent corrector sequences or not. When deciding which GREEN or YELLOW child nodes to keep, a more sophisticated criterion is applied that requires a few definitions.

Definition 3.1. A *path* P in the computation tree is a connected subtree in which each node has at most one child node.

A path in the computation tree corresponds to a putative segment of the continuation curve. An ordered sequence of connected nodes (*e.g.*, $P = (\alpha_1, \alpha_2, \dots, \alpha_N)$) represents a path in the computation tree.

Being able to identify paths in the computation tree, there are two important measures needed to control our algorithm.

Definition 3.2. The *initialization length* of the path $P = (\alpha_1, \alpha_2, \dots, \alpha_N)$ is

$$L(P) = \sum_{k=1}^N h_{\alpha_k}^{\text{init}}. \quad (5)$$

Definition 3.3. The *iteration cost* of the path $P = (\alpha_1, \alpha_2, \dots, \alpha_N)$ is

$$I(P) = \mu_{\alpha_1} \text{ where } \mu_{\alpha_k} = \begin{cases} \nu_{\alpha_k}, & \text{if } k = N, \\ \max(\nu_{\alpha_k}, \mu_{\alpha_{k+1}} + \nu_{\alpha_{k+1}}^{\text{init}}), & \text{otherwise.} \end{cases} \quad (6)$$

That is, $L(P)$ is the pseudo-arclength of the segment of the curve associated with the nodes of P in sequence—assuming the points associated with the nodes all lie on the continuation curve. Similarly, $I(P)$ is the accumulated number of corrector steps computed to attain the current state of the entire path.

It is useful to identify two specific kinds of paths in the tree to choose between “converged” and “nearly converged” corrector sequences (represented on the tree by GREEN and YELLOW nodes, respectively).

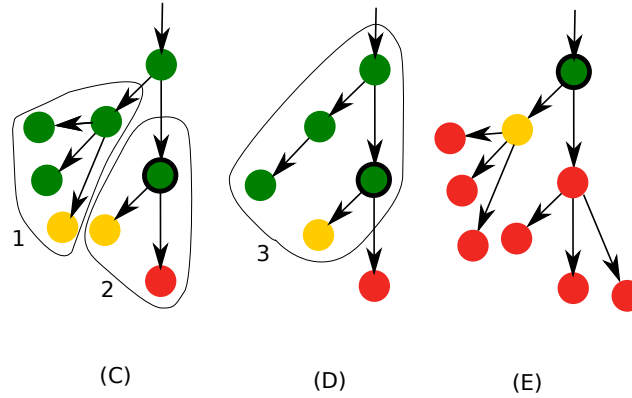


Fig. 2. Illustration of the pruning algorithm on a tree of width 3 and depth 3. For each subtree, the path that is expected to yield the fastest progress is retained with any RED nodes. This path is first selected in the smaller subtrees 1 and 2 and then in the larger subtree 3. After pruning, the GREEN node at the root of subtree 2 in panel (C) becomes the new root node and three new leaves are spawned from both of its children (as shown in panel (E)).

Definition 3.4. A *valid path* is a path in which all nodes are GREEN.

Definition 3.5. A *viable path* is a path in which all nodes are either GREEN or YELLOW.

Notice a valid path is, by definition, a viable path also.

Thus, before the second stage of pruning, valid and viable paths are identified recursively (line 12 of Algorithm 3). Naturally, a valid path comprises nodes associated with points known to be on the continuation curve (within the desired tolerance). Viable paths consist of nodes associated with points that are either known to be on the continuation curve or points that are likely to be on the curve in the next concurrent corrector iteration. As such, when comparing a node's GREEN and YELLOW child nodes, Algorithm 4 chooses the node associated with the longest viable or valid path (measured in pseudo-arclength).

In the event that distinct valid and viable paths exist, Algorithm 4 decides whether to keep the best valid or the best viable path. In particular, to choose between the longest valid path $P_{\text{valid}}(\alpha)$ and the longest viable path $P_{\text{viable}}(\alpha)$ extending below node α , the rate of progress along the curve is estimated by computing

$$\frac{L(P_{\text{valid}}(\alpha))}{I(P_{\text{valid}}(\alpha))} \quad \text{and} \quad \frac{L(P_{\text{viable}}(\alpha))}{I(P_{\text{viable}}(\alpha)) + 1}. \quad (7)$$

The algorithm keeps whichever child node leads to the path with the greatest rate of progress as computed in (7); the other GREEN and YELLOW child nodes are deleted (with their associated subtrees).

Figure 2 illustrates Algorithm 4 for a tree of width 3 and depth 3 continuing where Figure 1 stopped. The step lengths in this example are $\{t_k\}_{k=1}^W = \{1/4, 1, 3/2\}$. In panel (C), the root GREEN node represents a solution that has been computed after two corrector steps, while its child nodes have been spawned after one step. First, subtrees 1 and 2 are examined to choose which child to keep. Subtree 2 in panel (C) has only a single viable path, so it is left alone. Subtree 1 in panel (C) has two valid and three viable paths from its root GREEN node. The longest valid and longest viable paths are compared using (7) and only the path with the greatest “speed” is kept. The longest valid path took two corrector steps to construct and gives a gain of $t_1h + t_2t_1h = h/2$ in arc length, while the longest viable path is expected to yield a gain of $t_1h + t_3t_1h = 5h/8$

in three steps. Since $(h/2)/2 > (5h/8)/3$, the longest valid path is retained. The result in panel (D) is subtree 3 hanging off the root GREEN node which has one valid and two viable paths. Here, retaining the all-green (valid) subtree, on the left, would lead to a gain of $(1 + t_1 + t_2 t_1)h = 3h/2$ in three corrector steps. Retaining the GREEN and YELLOW (viable but not valid) subtree, on the right, should give a gain of $(1 + t_2 + t_1 t_2)h = 9h/4$ in four corrector steps. Since $(3h/2)/3 = h/2 < 9h/16 = (9h/4)/4$, the the GREEN and YELLOW sub tree is retained. Subsequently, the next GREEN node on the retained path becomes the new root node in panel (E). The YELLOW and RED nodes from panel (D) are used to compute new predictor points in panel (E).

ALGORITHM 4: PruneTree(α_r)

Input: root node α_r of computation tree

- 1 **foreach** node α in a depth-first traversal of computation tree rooted at α_r **do**
- 2 | **if** $c_\alpha = \text{BLACK}$ **then**
- 3 | | delete subtree rooted at α
- 4 **foreach** node α in a depth-first traversal of computation tree rooted at α_r **do**
- 5 | compute paths $P_{\text{viable}}(\alpha)$ & $P_{\text{valid}}(\alpha)$, the respective viable and valid paths of longest initialization path length rooted at node α
- 6 **foreach** node α in a depth-first traversal of computation tree rooted at α_r **do**
- 7 | $P_{\text{best}}(\alpha) \leftarrow \emptyset$
- 8 | **if** $P_{\text{viable}}(\alpha) \neq \emptyset$ **then**
- 9 | | $P_{\text{best}}(\alpha) \leftarrow P_{\text{viable}}(\alpha)$
- 10 | | **if** $P_{\text{valid}}(\alpha) \neq \emptyset$ and $P_{\text{valid}}(\alpha) \neq P_{\text{viable}}(\alpha)$ **then**
- 11 | | | $S_{\text{valid}}(\alpha) \leftarrow L(P_{\text{valid}}(\alpha))/I(P_{\text{valid}}(\alpha))$
- 12 | | | $S_{\text{viable}}(\alpha) \leftarrow L(P_{\text{viable}}(\alpha))/[I(P_{\text{viable}}(\alpha)) + 1]$
- 13 | | | **if** $S_{\text{valid}}(\alpha) \geq S_{\text{viable}}(\alpha)$ **then**
- 14 | | | | $P_{\text{best}}(\alpha) \leftarrow P_{\text{valid}}(\alpha)$
- 15 | **foreach** child node β of node α **do**
- 16 | | **if** $\beta \notin P_{\text{best}}(\beta)$ and $c_\beta \in \{\text{YELLOW}, \text{GREEN}\}$ **then**
- 17 | | | delete subtree rooted at β
- 18 **return**

4. STRUCTURE OF THE CODE

We have implemented the algorithms from Section 3 in a library called PAMPAC (Parallel Adaptive Method for Pseudo-Arclength Continuation). The PAMPAC library is written in C (ISO/IEC 9899:1999) using MPI-2 libraries (the Message Passing Interface, see [Gropp et al. 1999]) for parallelization. The main PAMPAC library comes with template Makefiles for easy building; some configuration of the file Makefile.in may be required to ensure that all library dependencies are met on a user's system, but the goal is straightforward and builds on any POSIX system. The code is packaged with an example (described more fully in Section 5.1) to help users modify their own continuation codes for use with PAMPAC easily.

To use the PAMPAC library, the user needs to supply:

- a main function (usually in a file main.c) to drive the computation;
- a C function compute_residual that evaluates $F(z)$ in (1);

- a C function `single_corrector_step` that computes the updated corrector iterate $\zeta_{\alpha}^{(\nu_{\alpha}+1)}$ from $\zeta_{\alpha}^{(\nu_{\alpha})}$ and \mathbf{T} as required in line 7 of Algorithm 2 for pseudo-arclength continuation; and
- an input file (ASCII text) containing the initial data point $\mathbf{z}^* = (\mathbf{x}^*, \lambda^*)$ on the continuation curve.
- a parameter file (usually `parameters.txt`) for tuning the behavior of Algorithm 3.

The subdirectory of `examples` contains a template file `main.c` that can be used with little or no modification. That directory also contains a sample `parameters.txt` file for controlling the algorithm behavior. The code is modular to aid in debugging and understanding; each of the core tasks listed in Algorithm 3 of Section 3 is performed by a separate function.

The main function performs two primary tasks: it initializes and finalizes MPI communication and it divides work between the master and the slave processes (this is typical in the Single-Program-Multiple-Process (SPMP) paradigm). The master processor parses the user-provided parameter file to determine the algorithm-tuning parameters and calls the routine `master_process`; this routine does some preprocessing (e.g., loading the initial point from the user’s input file and computing an initial tangent direction) before initiating Algorithm 3. The slave processes all call the function `slave_process` in which they idle until receiving data from the master process—the data being a point $\zeta \in \mathbb{R}^{n+1}$ and some tangent direction $\mathbf{T} \in \mathbb{R}^{n+1}$ from which a corrector iteration can be computed. The only interprocess communication during the continuation loop consists of the root process sending these data to the slaves and each slave returning the result of a corrector step to the root process. The routines `master_process` and `slave_process` package the core components of Algorithm 3 in a manner that alleviates the burden of managing the parallel computation from the user. As mentioned in Section 3, the corrector iterations are independent and are generally much more expensive than the cost of inter-process communication.

The user-supplied routines `compute_residual` and `single_corrector_step` have the following C function prototypes:

```
void compute_residual (int N_dim, const double* z, double* residual);
void single_corrector_step (int N_dim, double* zeta, double* Tangent);
```

Both functions do not have return values; rather, the “output” values computed are passed by reference (a common idiom in C and FORTRAN programming). Notice that, relative to the mathematical description of the template continuation problem in Section 2, `N_dim` = $n + 1$, i.e., `N_dim` refers to the dimension of the vector $\mathbf{z} = (\mathbf{x}, \lambda)$ rather than the dimension of the vector \mathbf{x} . Thus, in `compute_residual`, the “input” values are the (integer) dimension `N_dim` of the problem and the `N_dim`-vector pointed to by the pointer `z`; the “output” is the residual vector $\mathbf{F}(\mathbf{z})$ in (1) stored in an array of length `N_dim-1` in memory pointed to by the pointer `residual`. Similarly, in `single_corrector_step`, the “input” values are the (integer) dimension `N_dim` of the problem, the `N_dim`-vector pointed to by the pointer `zeta`, and the `N_dim`-vector pointed to by the pointer `Tangent` (corresponding to \mathbf{T}). After calling `single_corrector_step`, the array pointed to by `zeta` has been overwritten with the updated corrector iterate as in Algorithm 2. These functions need to be compiled with `main.c`—and any user-required dependencies—to produce an executable that can be run in parallel on numerous processors. Assuming that the user’s `Makefile` is suitably configured, the user can link the executable with external library functions required by their routines.

Parameters controlling the parallel continuation Algorithm 3 are loaded from a plain text file at run-time by the master processor. The user needs to provide the following values:

- N_DIM: the number of unknowns $n + 1$;
- LAMBDA_MIN and LAMBDA_MAX: bounds on the interval $[\lambda_{\min}, \lambda_{\max}]$ in which the continuation parameter λ lies;
- LAMBDA_INDEX: integer between 0 and N_DIM-1 that is the index of the parameter λ in any N_DIM-vector;
- DELTA_LAMBDA: parameter for initial corrector iterations to generate a second point on the curve from the first (required to bootstrap the algorithm);
- H_MIN, H_MAX and H_INIT: the minimal, maximal and initial pseudo-arclength step-size;
- MAX_ITER: the maximum number of corrector steps before coloring a node BLACK;
- TOL_RESIDUAL: the threshold residual tolerance in Eq. 1 for accepting GREEN nodes (*i.e.*, when $\|\mathbf{r}_\alpha^{(\nu_\alpha)}\| \leq \text{TOL_RESIDUAL}$);
- MU: the threshold reduction in residual for BLACK nodes (*i.e.*, when $\|\mathbf{r}_\alpha^{(\nu_\alpha)}\| > \text{MU} \|\mathbf{r}_\alpha^{(\nu_{\alpha-1})}\|$);
- GAMMA: the threshold rate of residual reduction for YELLOW nodes (*i.e.*, when $\text{GAMMA} \log \|\mathbf{r}_\alpha^{(\nu_\alpha)}\|^2 \leq \log \text{TOL_RESIDUAL}$);
- MAX_DEPTH: the maximum depth of the tree, D ;
- MAX_CHILDREN: the maximum width of the tree, W ;
- SCALE_PROCESS_K ($K = 0 \dots W - 1$): the step-size scalings t_K in Algorithm 3; and
- VERBOSE: an integer parameter controlling verbose output.

Certain parameters in the user's parameter file are not mentioned in the description of Algorithm 3 from Section 3. To circumvent a stagnating loop, the user can specify a positive integer MAX_ITER to terminate corrector iterations. The parameter LAMBDA_INDEX provides additional flexibility by permitting the user to specify any integer index of \mathbf{z} —using 0-based indexing as is conventional in C—for the continuation parameter. That is, the parameter λ does not need to be the $(n + 1)^{\text{st}}$ component of the $(n + 1)$ -vector \mathbf{z} .

To bootstrap Algorithm 3, the master processor requires an initial tangent direction in addition to the initial point loaded from the user's input file. It generates an approximate tangent direction by carrying out a few corrector iterations to generate another point near the initial point and computing a secant direction between those two points. At any given point on the continuation curve, there are two anti-parallel tangent directions; as such, the sign of H_INIT is used to fix the initial direction of the continuation (*i.e.*, the tangent direction used to generate the second point on the curve is oriented in the direction of λ increasing or decreasing when $\text{H_INIT} > 0$ or $\text{H_INIT} < 0$, respectively). The user also needs to specify DELTA_LAMBDA (roughly how far from the initial point to look for the neighboring point) to control this bootstrapping process.

Finally, the user can specify an integer parameter VERBOSE to control output generated at run-time. No output is generated unless the parameter VERBOSE is positive; With $\text{VERBOSE} \geq 1$, the master process displays diagnostic messages to standard output as the algorithm progresses. When $\text{VERBOSE} \geq 2$, the master process also creates data files in a user-specified path that display the structure of the rooted trees. The data files generated are compatible with the dot language for specifying directed graphs with the GRAPHVIZ software for visualization of graphs (see www.graphviz.org). Such graphs are useful for performance-tuning, *i.e.*, for understanding how the data in parameters.txt affect the use of processors.

Many of the core routines in the PAMPAC library require traversal of the rooted tree in a depth-first (using recursion) or a breadth-first (using a queue) fashion. The node and queue data structures for managing the tree are documented in pampac.h in the src subdirectory. This file also describes a data structure for storing and communicating the parameter options parsed from the user's parameter file. The PAMPAC library

is designed so that users need not know the details of the implementations of these data structures (nor the routines for allocation/deallocation of memory, management of pointers, etc.). The user need only specify the width and depth of the underlying tree and the related tunable parameters that control the parallel algorithm.

5. NUMERICAL EXAMPLES

We present two examples to test the performance of the parallel algorithm. The first example concerns travelling waves in a 1 + 1 dimensional, nonlinear, partial differential equation (PDE) and is distributed with the PAMPAC library in the `examples` directory. The second concerns time-periodic solutions to the Navier-Stokes equation on a three-dimensional, periodic domain. In both test cases, the number of unknowns is in the thousands, but the corrector step is computed differently. In the first test case, we compute and LU-decompose the dense Jacobian matrix, while in the second case, an inexact Krylov subspace method is used. An additional difference is that the first test case was implemented in C, but needs to be linked to external numerical libraries, whereas the second is a self-contained legacy FORTRAN code. In spite of these differences, a similar set of parameters gives rise to similar speed-up.

5.1. Travelling waves in a modified Kuramoto-Sivashinsky equation

The Kuramoto-Sivashinsky equation was derived independently in different contexts, most notably by Kuramoto and Tsuzuki [1976] for describing phase dynamics in reaction-diffusion systems and by Sivashinsky [1977] for describing flame front dynamics. The similarity of its quadratic nonlinearity to that of the Navier-Stokes equation makes it a popular test case for numerical methods for PDEs. We add a second nonlinear term to obtain

$$u_t + uu_x + u_{xx} + \lambda u_{xxxx} - A \sin(u) = 0 \quad (8)$$

The extra nonlinear term breaks the equivariance under Galileo boosts so that we can compute families of travelling waves with a uniquely determined wave speed. The modified equation is still equivariant under translations and under the reflection symmetry given by $S : (u, x) \rightarrow (-u, -x)$.

We consider this PDE on a periodic domain, i.e. $u \in C^4(S)$, fixing $A = 8.09$ and considering the viscosity, $\lambda > 0$, as control parameter. There is always a trivial solution at $u \equiv 0$, from which equilibria branch off with increasing wave number for decreasing viscosity. In Fig. 3 a branch with wave number two is shown. This branch is symmetric under the reflection S , as well as under the shift \mathcal{T} over half the domain. At $\lambda \approx 0.48$, a family of equilibria branches off in a bifurcation that breaks the translational symmetry. Subsequently, at $\lambda \approx 0.18$, a family of travelling waves is created, shown in detail in Fig. 4.

This family has a number of fold points and the wave changes its shape rapidly along the branch. Therefore, its computation by the traditional pseudo-arclength continuation approach suffers from many failed steps. Moreover, the wave becomes increasingly localized for small values of the viscosity. In order to resolve it correctly, we need fine discretization, which will result in time-consuming corrector steps.

We compute the travelling waves as $u(x, t) = w(x - ct)$, which results in the following Boundary Value Problem (BVP):

$$-cw' + ww' + w'' + \lambda w'''' - A \sin(w) = 0; \quad w(0) = w(2\pi)$$

The linear terms in this equation are efficiently computed in Fourier space, while the nonlinear terms are best computed on a regular, periodic grid. Thus, we approximate

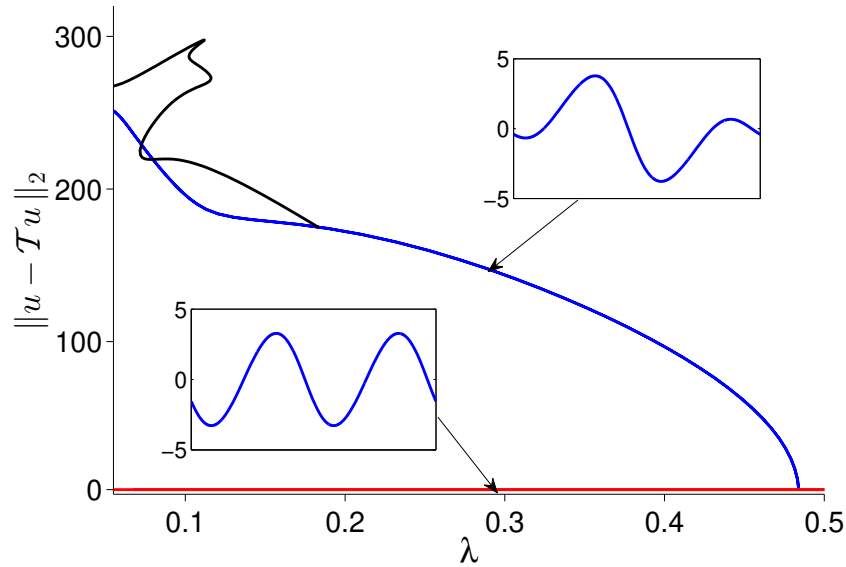


Fig. 3. Partial bifurcation diagram of the discretization of PDE model 8. In red: branch of equilibria invariant under symmetries \mathcal{S} and \mathcal{T} . In blue: branch of equilibria invariant only under \mathcal{S} . In black the branch of travelling wave solutions shown in detail in Fig. 4. Shown is a measure for the deviation from invariance under the shift \mathcal{T} versus the viscosity.

solutions as

$$w_j = \sum_{k=0}^{n-1} a_k e^{ikx_j}, \text{ where } x_j = \frac{2\pi}{n}j, j = 0, \dots, n-1$$

and switch between the representations $\{w_j\}$ and $\{a_k\}$ by the discrete Fourier transform, implemented using the FFTW library [Frigo et al. 2005]. The computational cost of each transform is $O(n \ln n)$. The resolution is fixed to $n = 2048$, fine enough to resolve the solutions shown in Fig. 4 and avoid aliasing issues.

The continuation problem now takes the form $F(a_0, \dots, a_{n-1}, c, \lambda) = 0$, where F and its derivatives are evaluated using the pseudo-spectral method outlined above. Since we have an extra unknown, the wave speed c , we must add an extra equation to ensure uniqueness of the corrector steps. We impose that the Newton update steps be orthogonal to w_x , the generator of the symmetry group of translations. This condition ensures that the successive iterates under corrector steps do not slide along the x -direction. Because of the second nonlinear term in Eq. 8, the Jacobian matrix F_x is dense. The test code takes $O(n^2)$ flops to compute this matrix and a further $O(n^3)$ flops to LU-decompose it when solving for the Newton update step. Thus, the execution of a single Newton step in this test has a complexity of $O(n^3)$ and takes a few seconds on a single, 2.2GHz CPU, rendering the MPI communication time negligible. In Table I all parameters relevant for the numerical computation are given.

The wall time for the computation of the entire curve shown in Fig. 4 using various tree structures and step-size distributions is shown in Fig. 5. The maximal speed-up is about a factor of three, obtained with a tree depth and width of three. In that computation, there is a lot of redundancy as many processors will be working on very

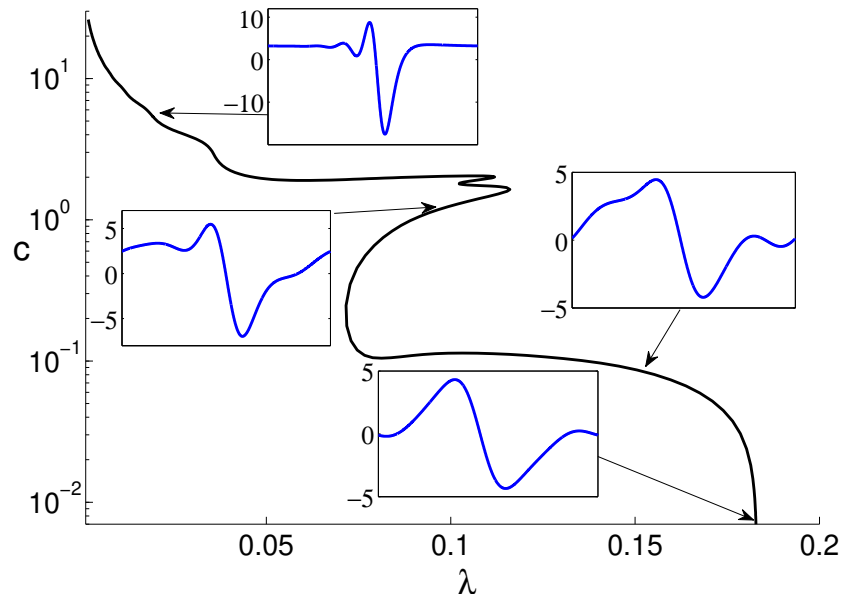


Fig. 4. The branch of travelling wave solutions to Eq.8 used for testing the parallel continuation algorithm. Shown is the wave speed, c , versus the control parameter, λ . The inlays show snapshots of the solution $u(x, t)$ at four points along the continuation curve. At $c = 0$, the wave bifurcates from an equilibrium, which is symmetric under the reflection symmetry. For $\lambda \lesssim 0.01$ the solution becomes strongly localized.

Table I. System and algorithm parameters for the numerical experiments with the modified Kuramoto-Sivashinsky equation.

A	8.09	amplitude of second nonlinear term
$[\lambda_0, \lambda_1]$	[0.1828, 0.001]	range of the continuation parameter
n	2048	# grid points
$\{t_i\}_{i=1}^3$	{0.75, 1, 2}	step-size multipliers
H_{\max}	2000	maximal step size
H_{\min}	10^{-2}	minimal step size
H_{init}	100	initial step size
ν_{\max}	4	maximal number of Newton iterations
μ	0.5	minimal linear residual decrease
γ	2.0	expected order of residual decrease
r_{\max}	$5 \cdot 10^{-7}$	tolerance for the nonlinear problem

similar approximate solutions. A speed-up of more than a factor of two, however, can be obtained using as few as three processors with the same step-size multiplication factor. The three depth seems to impact the efficiency much more strongly than the tree width, but this is likely problem-dependent. Some initial experimentation will be necessary for each individual problem to determine a near-optimal strategy for a given number of available processors.

5.2. Periodic solutions in a turbulent flow

The second test problem concerns the continuation of time-periodic solutions to the Navier-Stokes equation for fluid motion. We consider an incompressible, viscous fluid in a box with periodic boundary conditions in every direction. In the simulation code, the unknown variables are the Fourier coefficients of the vorticity field, truncated to

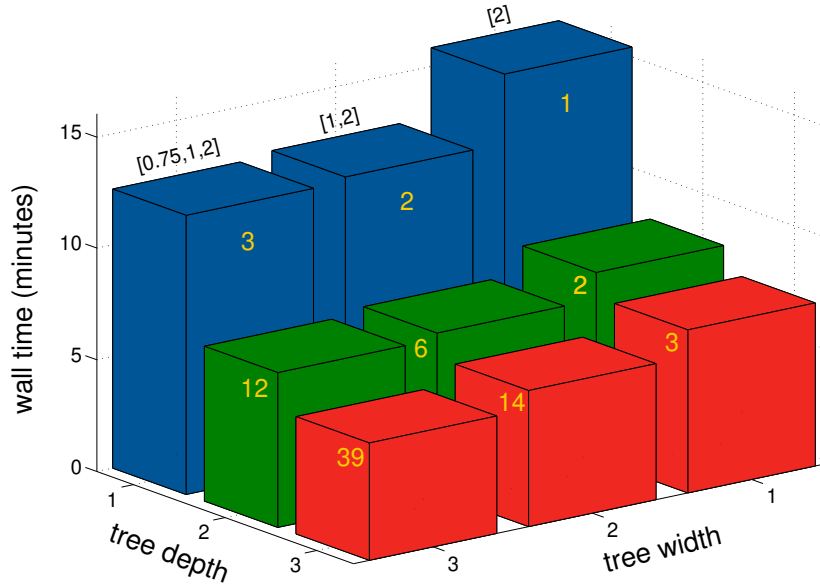


Fig. 5. Wall time for the computation of the continuation curve shown in Fig. 4 using a tree width and depth up to three. The numbers between brackets denote the multipliers for the step-size, $\{t_i\}_{i=1}^W$ and the integer denotes the number of CPUs concurrently processing corrector steps.

a finite number. Energy is input by keeping fixed in time some coefficients with small wave numbers, corresponding to large spatial scales. At small spatial scales, energy is dissipated by viscous processes. The resulting turbulent flow is statistically stationary and exhibits a cascade of energy across spatial scales. Although the statistical description of this cascade is well developed (see, e.g., [Monin and Yaglom 2007, Ch. 7]), the dynamics of this process are largely unknown.

In van Veen et al. [2006], time-periodic solutions of this flow are considered as building blocks of turbulence. The idea is to study the dynamics and parameter dependence of such building blocks and distill from the results a hypothesis on the dynamical processes that contribute to the energy cascade. The essential difficulty in computation is that a very large number of degrees of freedom is required to simulate of the flow accurately. Even for weakly turbulent flow, about $n \simeq 10^6$ degrees of freedom are needed; this number increases algebraically with Taylor's microscale Reynolds number, Re_λ , which, in turn, increases with decreasing viscosity. Symmetry arguments reduce the number of degrees of freedom to $n \simeq 10^4$, thereby making the study of the resulting *high symmetric flow* feasible [Kida 1985].

After symmetry reduction, the resulting system is a set of n coupled, nonlinear ODEs with a single parameter, namely the kinematic viscosity, here denoted by λ , which determines the Reynolds number of the flow. Time-stepping is done by the pseudo-

Table II. System and algorithm parameters for the numerical experiments with high-symmetric flow.

$[\lambda_0, \lambda_1]$	$[0.0045, 0.0035]$	range of the continuation parameter
N	128^3	spatial resolution
n	6370	# variables
$\{t_i\}_{i=1}^3$	$\{0.75, 1, 2\}$	step-size multipliers
h_i	0.01	initial step-size
q	0.5	minimal residual decrease is $\ r^{(\alpha, \nu_\alpha)}\ _2 < q \ r^{(\alpha, \nu_\alpha - 1)}\ _2$
t_f	0.5	step-size multiplier if all child nodes fail
TOL	10^{-6}	tolerance for the nonlinear problem
GMRESTOL	10^{-5}	relative residual tolerance for GMRES
Δt	5×10^{-3}	step-size for 4 th order Runge-Kutta-Gill time stepping

spectral method, employing the fourth-order Runge-Kutta-Gill scheme. In the results presented here, the spatial resolution is fixed at 2^7 points in every direction which, after de-aliasing and symmetry reduction, gives $n = 6370$ variables. The kinematic viscosity is varied in the range $0.0045 \geq \lambda \geq 0.0035$, which corresponds to a Taylor microscale Reynolds number Re_λ in the range $57 \leq Re_\lambda \leq 68$. The square of this dimensionless number can be compared to the commonly used geometric Reynolds number Re .

Periodic solutions are computed as fixed points of an iterated Poincaré map, i.e., as solutions of a nonlinear system

$$\mathcal{P}^{(k)}(\mathbf{x}, \lambda) - \mathbf{x} = \mathbf{F}(\mathbf{x}, \lambda) = \mathbf{0}. \quad (9)$$

In (9), \mathbf{x} is the vector of Fourier coefficients of the vorticity field and k is the discrete period of the orbit. The Poincaré plane of interesection is a coordinate plane on which one of the low wavenumber Fourier coefficients equals its time-averaged value. A solution of discrete period $k = 5$ is filtered from turbulent data at the highest viscosity. At this viscosity, the flow is relatively quiescent. Subsequently, pseudo-arclength continuation is used to track the periodic solution to the more turbulent regime. In the correction step of pseudo-arclength continuation, the linear problem associated with the Newton-Raphson iteration is solved in an inner Generalised Minimal Residual (GMRES) iteration [Saad and Schultz 1986]. The combination of pseudo-arclength continuation with a Krylov subspace iteration is called *Newton-Krylov continuation* and was first implemented by Sánchez et al. [2004]. Each linear problem within this continuation takes about twenty inner GMRES iterations to solve. In turn, each inner GMRES iteration requires integrating a system of n ODEs modeling the flow along an approximately periodic orbit. On a single, 2.2GHz CPU, one corrector step takes about 13 minutes, again rendering the MPI communication time negligible. All system and algorithm parameters used to generate the results below are listed in Table II.

Figure 6 shows the numerical curve produced by pseudo-arclength continuation. The points shown are computed using a naive scheme for step-size control: the step-size is doubled after each successful step, halved after each failed step. Twelve points are computed along the curve at the cost of fifty-five Newton-Krylov iterations. Out of these fifty-five correction steps, fifteen steps were rejected; thus, over a quarter of the time (as measured on a wall-clock) was wasted. A more careful strategy based on a local estimate of the curvature yields eighteen points computed on the numerical curve at a cost of forty-nine Newton iterations with four rejected steps. In Fig. 7 the wall time required by PAMPAC is shown for tree configurations up to width and depth three. As compared to the first test case, the tree width, i.e. the number of different step lengths attempted in parallel, is of greater influence. However, a speed-up by a factor of two is again obtained using three CPUs and the maximal speed-up by a factor of three is obtained on 39 CPUs.

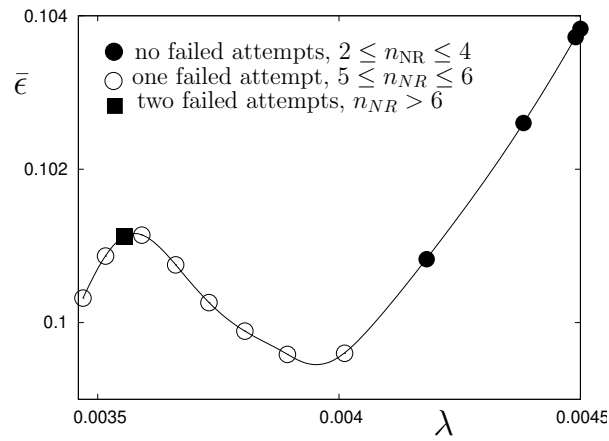


Fig. 6. Continuation of a periodic solution in high-symmetric flow by serial pseudo-arclength continuation. Dots, circles, and squares denote points computed after zero, one and two failed correction steps, respectively.

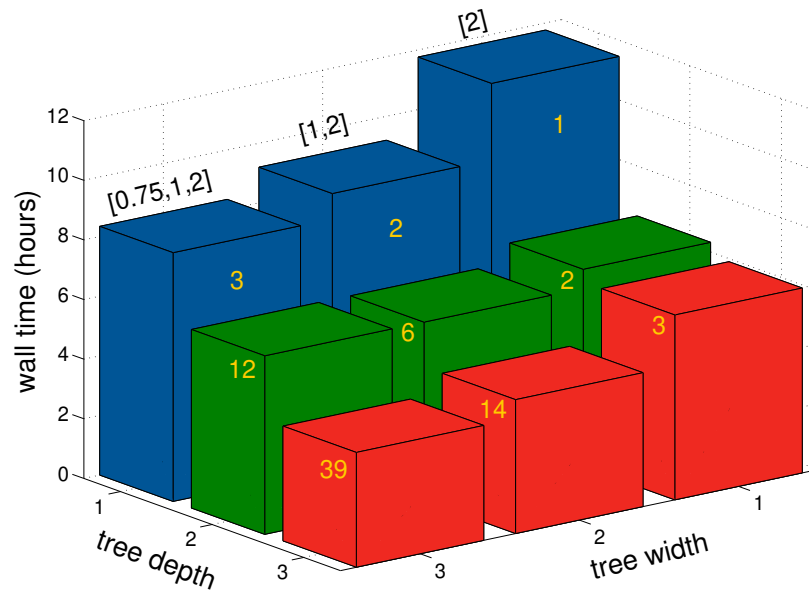


Fig. 7. Wall time in hours versus tree width and depth. The numbers between brackets are the step length multiplication factors $\{t_i\}_{i=1}^W$ and the integer on each data bar is the number of CPUs concurrently processing corrector steps.

6. CONCLUSION

In the computation of parametrised solutions to discretised PDEs, most elements have been optimised for efficiency. For instance, when studying Navier–Stokes flow, we often use pseudo-spectral time-stepping in combination with fast Fourier transforms. The linear systems we must solve to find Newton update steps are handled by Krylov subspace methods, whose convergence can be sped up by a host of preconditioners. In contrast, the continuation algorithm, which forms the outer loop of the computation, is essentially the same as that used for small sets of ODEs. For such small systems, selecting an unnecessarily small step-size, or a overly large step-size that leads to diverging corrector steps, will cost seconds or minutes of computation time. For large systems, this may cost days or weeks.

In this paper, we have presented an elegant, recursive algorithm that combines two strategies for aggressively optimising the step-size and minimising the computation time. The first is to try several step-sizes in parallel, and the second is to predict new solutions from a sequence of corrector steps, before this sequence has converged.

Two test cases, different in the type of solution computed, the linear solving and the implementation, demonstrate that the continuation can be sped up by a factor of two using only three processors, and by a factor of three using thirty nine. Since multi-core processors are a standard feature of new desktop computers, and cluster computers are available in many places, we expect that our algorithm will be useful to many researchers working on nonlinear problems with many unknowns.

ACKNOWLEDGMENTS

The computations presented in Sec. 5 were made possible by the facilities of the Shared Hierarchical Academic Research Computing Network (SHARCNET:www.sharcnet.ca) and Compute/Calcul Canada.

REFERENCES

- ALLGOWER, E. L. AND GEORG, K. 2003. *Introduction to Numerical Continuation Methods*. Classics in Applied Mathematics Series, vol. 45. SIAM, Philadelphia.
- ANDERSON, E., BAI, Z., BISCHOF, C., BLACKFORD, S., DEMMEL, J., DONGARRA, J., DU CROZ, J., GREENBAUM, A., HAMMARLING, S., MCKENNEY, A., AND SORENSEN, D. 1999. *LAPACK Users' Guide* Third Ed. SIAM, Philadelphia, PA.
- DICKSON, K., KELLEY, C., IPSEN, I., AND KEVREKIDIS, I. 2007. Condition Estimates for Pseudo-arclength Continuation. *SIAM J. Numer. Anal.* 45, 1, 263–276.
- DOEDEL, E., CHAMPNEYS, A., DERCOLE, F., FAIRGRIEVE, T., KUZNETSOV, Y. A., OLDEMAN, B., PAFFENROTH, R., SANDSTEDTE, B., WANG, X., AND ZHANG, C. 2008. *AUTO-07P: Continuation and bifurcation software for ordinary differential equations*. Concordia University, Montreal, Canada. Available from <http://sourceforge.net/projects/auto-07p/>.
- FRIGO, M., STEVEN, AND JOHNSON, G. 2005. The design and implementation of FFTW3. In *Proceedings of the IEEE*. 216–231.
- GOVAERTS, W. 2000. *Numerical Methods for Bifurcations of Dynamic Equilibria*. SIAM, Philadelphia.
- GROPP, W., LUSK, E., AND THAKUR, R. 1999. *Using MPI-2: Advanced Features of the Message-Passing Interface*. MIT Press, Cambridge, MA, USA.
- KAWAHARA, G., UHLMANN, M., AND VAN VEEN, L. 2012. The significance of simple invariant solutions in turbulent flows. *Ann. Rev. Fluid Mech.* 44, 203–225.
- KELLER, H. 1977. Numerical Solution of Bifurcation and Nonlinear Eigenvalue Problems. In *Applications of Bifurcation Theory*, P. Rabinowitz, Ed. Academic Press, New York, 359–384.

- KELLEY, C. 2003. *Solving Nonlinear Equations with Newton's Method*. Fundamentals of Algorithms. SIAM, Philadelphia.
- KIDA, S. 1985. Three-dimensional periodic flows with high-symmetry. *J. Phys. Soc. Japan* 54, 2132–2136.
- KNOLL, D. AND KEYES, D. 2004. Jacobian-free Newton-Krylov methods: a survey of approaches and applications. *J. Comp. Phys.* 193, 1, 357–397.
- KURAMOTO, Y. AND TSUZUKI, T. 1976. Persistent propagation of concentration waves in dissipative media far from thermal equilibrium. *Prog. Theor. Phys.* 55, 356–369.
- KUZNETSOV, Y. 1998. *Elements of Applied Bifurcation Theory*. Springer-Verlag, New York.
- MONIN, A. S. AND YAGLOM, A. M. 2007. *Statistical fluid mechanics, volume 2*. Dover publications, New York.
- SAAD, Y. AND SCHULTZ, M. 1986. GMRES: A Generalized Minimal Residual Algorithm for Solving Nonsymmetric Linear Systems. *SIAM J. Sci. and Stat. Comput.* 7, 856–869.
- SÁNCHEZ, J., NET, M., GARCÍA ARCHILLA, B., AND SIMÓ, C. 2004. Newton-Krylov continuation of periodic orbits for Navier-Stokes flows. *J. Comp. Phys.* 201, 1, 13–33.
- SIVASHINSKY, G. 1977. Nonlinear analysis of hydrodynamic instability in laminar flames I. derivation of basic equations. *Acta Astron.* 4, 1177–1206.
- VAN VEEN, L., KIDA, S., AND KAWAHARA, G. 2006. Periodic motion representing isotropic turbulence. *Fluid Dyn. Res.* 38, 19–46.
- YANG, Z.-H. AND KELLER, H. 1986. A Direct Method for Computing Higher Order Folds. *SIAM J. Sci. Stat. Comput.* 7, 2, 351–361.

Received September 2013; revised ; accepted